Available online at www.sciencedirect.com
ScienceDirect
Journal of the European Ceramic Society 28 (2008) 1613–1621
www.elsevier.com/locate/jeurceramsoc

Liquid phase assisted hot pressing of boron suboxide-materials

A. Andrews [a], M. Herrmann [b,*], T.C. Shabalala [a], I. Sigalas [a]

[a] *School of Chemical and Metallurgical Engineering, University of the Witwatersrand, Private Bag 3, Wits 2050, Johannesburg, South Africa*
[b] *Fraunhofer Institute of Ceramic Technologies and Systems (IKTS), Winterbergstrasse 28, D-01277 Dresden, Germany*

Received 27 June 2007; received in revised form 15 September 2007; accepted 12 October 2007
Available online 28 January 2008

Abstract

B_6O composites were prepared by hot pressing of B_6O powder with alumina, aluminium and carbon additions. Dense materials with hardness higher than 30 GPa and fracture toughness of 3 MPa $m^{1/2}$ were achieved at 1900 °C. The sintering behaviour and the formed phases were discussed on the bases of thermodynamic calculations. The thermodynamic properties of boron suboxide (B_6O) were approximated at high temperatures. The phase equilibria computed based on the obtained thermodynamic properties, agree with the available experimental data. The modelled thermodynamic properties of B_6O have been applied to analyse interpretation of the sintering behaviour and the stability of these materials. The thermodynamic calculations and microstructural analysis showed that the densification takes place by liquid phase sintering.

Keywords: Boron suboxide; Thermodynamic properties; Liquid phase; Sintering; Hot pressing; B_6O

1. Introduction

The development of synthetic ultrahard materials which have hardness values approaching that of diamond-based materials has been of great interest. With Vickers hardness (H_v) of between 70 and 100 GPa, diamond is the hardest material known, followed by cubic boron nitride ($H_v \sim 60$ GPa) and boron suboxide ($H_v \sim 38$ GPa), herein referred to as B_6O.[1,2] The strong covalent bonds and short interatomic bond length contribute to a combination of unique properties, which are characteristic for many boron rich compounds.[1–6] Nevertheless boron suboxide, which can be produced and processed under ambient pressure, has not found industrial applications, due to the low fracture toughness and the lack of understanding of the relation between preparation, microstructure, and properties.

Boron suboxide-based compounds are normally densified at higher temperatures (≥1700 °C) and/or high pressures. There exist different approaches to produce these materials by reactive hot pressing of B_2O_3 and B or by hot pressing of B_6O powder.[1,2,7,8] All these materials had shown good microhardness values but their fracture toughness values were less than 2 MPa $m^{1/2}$.

Recently it was shown that the addition of Al or Al_2O_3 results in improved fracture toughness with only minor reduction in hardness.[7,9,10] Therefore a detailed understanding of the processes which take place during sintering would be helpful in the search of new additives for B_6O materials. A possible way for predicting the phase formation in B_6O composites during sintering is the thermodynamic calculation of the equilibrium phases. However, current knowledge on the thermodynamic properties of boron suboxide is limited to temperatures of up to 800 K.[11–13] The entropy was determined to be $\Delta S_{298.15} = 39.91$ J/(mol K) and the enthalpy of formation as $\Delta H_f^{\theta}(B_6O, s, 298.15\,K) = -527 \pm 32$ kJ mol^{-1}.[11] The temperature dependent heat capacity was established for the temperature range 298.15–800 K as

$$C_p = 54.55936 + 17.263 \times 10^{-2}T - 28.2 \times 10^{5}T^{-2}\ \ (J/(mol\,K))^{12} \quad (1)$$

In this paper, on the basis of these data and the thermodynamic data of similar borides, the thermodynamic function of B_6O at high temperature will be estimated and used for the calculation of the phase composition of $B_6O/Al/Al_2O_3$ and of B_6O/C-composite materials. The results will be compared with existing

* Corresponding author. Tel.: +49 351 25 53 527; fax: +49 351 25 53 600.
E-mail address: Mathias.Herrmann@ikts.fraunhofer.de (M. Herrmann).

0955-2219/$ – see front matter © 2007 Elsevier Ltd. All rights reserved.
doi:10.1016/j.jeurceramsoc.2007.10.011

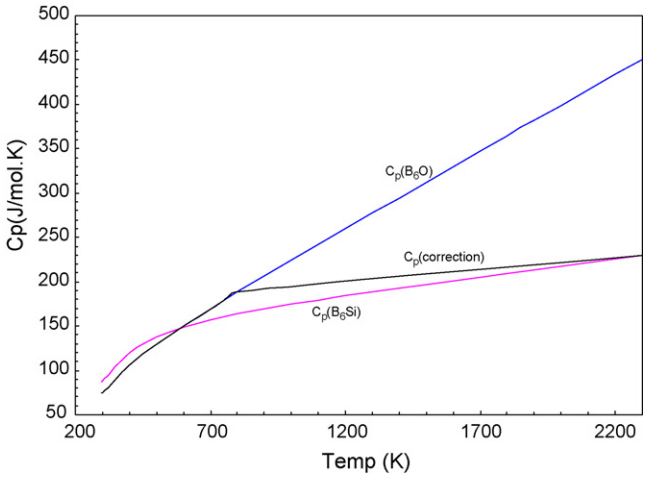

Fig. 1. Dependence of C_p vs. temperature for B_6Si, B_6O (extrapolated experimental values) and B_6O after correction (the data of B_6Si from **14**). The data of B_6O were measured in the range 298.15–800 K (**12**).

experimental data concerning different phase compositions of composites and used for explaining the sintering behaviour of B_6O-based materials.

2. Estimation of the Gibbs energy of B_6O

The Gibbs energy of B_6O can be calculated using the known standard enthalpy $\Delta H^{f}_{298.15}$ and entropy ($\Delta S_{298.15}$). Beside these values, the heat capacity is also necessary for the determination of the Gibbs energy ($G^{f}(T)$) at a higher temperature. These values are determined only up to 800 K and have to be estimated for higher temperatures.

The determined enthalpy of formation of B_6O agrees with other values for similar compounds such as B_6Si, B_6As, and B_6P.[11] Also the C_p values near room temperature are quite close to the C_p values of B_6Si (Fig. 1). This could be expected since the compounds have a similar structure, composition, and chemical bonding. The thermodynamic data for B_6Si were taken from FactSage™ Databank.[14] The extrapolation of the C_p values of B_6O to higher temperatures gives large differences between the two compounds (Fig. 1). Usually, the atomic heat capacities of all solid elements are in the range of $3R$ (=24.9 J/(mol K)) where R is gas constant (rule of Dulong and Pettit). Additionally, the molar heat capacity of a solid chemical compound is approximately equal to the sum of the molar heat capacities of its constituent chemical elements.[15] Using this rule the heat capacity of B_6Si can be estimated as 207.2 J/K compared to 217.223 J/K (FACT53) or 204.716 J/K (SGPS-Database) found in literature at 2000 K.[14] It follows that the maximum heat capacity of B_6O should be equal to the heat capacity of six boron atoms plus one oxygen atom, i.e. it has to be in the same region as B_6Si. Therefore, 213 J/K mol was chosen as the value at 2000 K and a linear C_p function above the measured range (781 K), was introduced to correct the deviation between the heat capacities of B_6O and B_6Si in the temperature range of 800–2300 K (Fig. 1). Therefore, C_p function used in this work was: $C_p = 54.56 + 17.263 \times 10^{-2}T - 28.2 \times 10^{5}T^{-2}$ (J/(mol K)) for $T < 800$ K[13] and $C_p = 0.023T + 166.54$ (J/(mol K)) for $T > 800$ K (determined by the approximation described).[2] Using the C_p values of B_6Si instead of the approximated B_6O, the Gibbs free energy of formation (ΔG) of B_6O would be somewhat lower, e.g. at 2000 K it would be −920.48 kJ/mol in comparison to −914.391 kJ/mol for the used dataset. This difference corresponds to an error of less than 1%. This difference can be viewed as the uncertainty of the determined values, even for B_6Si. The data do not take into account the fact that B_6O is normally non-stoichiometric.[16] The non-stoichiometry depends on synthesis conditions and is normally in the range of B_6O_x with $0.77 < x < 1$. However, no data concerning the dependence of thermodynamic data on the oxygen content in B_6O are known. The determination of the thermodynamic data[11–13] was carried out on materials produced at ambient pressure, and therefore it can be assumed that they have a similar non-stoichiometry as the powders used in this investigation.

Therefore in all calculations we assume the ideal composition of B_6O.

3. Experimental

The B_6O powders used were produced in laboratory scale as described in.[9,10] The mean grain size of the powder was in the range of 1 μm. The impurities introduced by the milling media was less than 0.2%. The determination of the content of B_2O_3 on the surface of the B_6O powder is difficult, because oxygen analysis of the materials does not give conclusive results due to the non-stoichiometry of the B_6O. The washing of the powder in hot alcohol reduces the B_2O_3 surface layer as was found for

Table 1
Phase composition, density and hardness of hot pressed samples prepared by admixing B_6O with Al powder and equilibrium phases calculated for the sintering temperature

Material name	Sintering conditions	Density (g/cm^3)	Knoop microhardness (GPa), 500 g	Crystalline phases formed after sintering	Thermodynamically calculated equilibrium phases
17-M5.2	1700 °C, 50 MPa, 20 min	1.33	–	B_6O, $Al_{18}B_4O_{33}$	B_6O, AlB_{12}, Al_2O_3
18-M5.2	1800 °C, 50 MPa, 20 min	2.30	18.0 ± 1.1	B_6O, $Al_{18}B_4O_{33}$	B_6O, AlB_{12}, Al_2O_3
19-M5.2	1900 °C, 50 MPa, 20 min	2.39	30.0 ± 0.9	B_6O, $Al_{18}B_4O_{33}$	B_6O, AlB_{12}, Al_2O_3
19-M7.3	1900 °C, 50 MPa, 20 min	2.35	26.0 ± 1.5	B_6O, $Al_{18}B_4O_{33}$, Al_2O_3	B_6O, AlB_{12}, Al_2O_3
19-M10	1900 °C, 50 MPa, 20 min	2.46	–	B_6O, Al_2O_3	B_6O, AlB_{12}, Al_2O_3
19B_6O	1900 °C, 50 MPa, 20 min	2.51	35.0 ± 0.8	B_6O	B_6O, AlB_{12}, Al_2O_3

The theoretical density of B_6O changes from 2.49 g/cm^3 for $B_6O_{0.76}$ to 2.53 g/cm^3 for $B_6O_{0.84}$ (ICSD 81-2192 and 87-2288).

B and BN powders.[19] The expected B_2O_3 content on the surface of the powder is assumed to be in the range of 1–2 wt.%. This is a common value for non-stable non oxide powders like SiC, BN, AlN of the same grain size.

Three sets of B_6O composite materials were prepared from these powders by hot pressing (HP20 Thermal Technology) at 1900 °C and at pressures of 50 MPa. The details of preparation are given elsewhere.[7,9,10]

The first set of materials was produced from the B_6O powder which was dry mixed with different amount of metallic aluminium (Saarchem; grain size of 5 μm) using a turbula mixer with Al_2O_3-balls for 2 h and then hot pressed in hBN lined graphite dies in Ar-atmosphere (Table 1). The addition of metallic Al was chosen to remove the remaining B_2O_3 in the sample.

The second set of samples was produced from the B_6O powders CVD coated with Al_2O_3. This was carried out by mixing B_6O and Al and NH_4Cl as reactive components and heating the mixture in a tube furnace under Ar at 1380 °C for 6 h.[7] The coating on the surface of B_6O particles was found to be mainly Al_2O_3; some traces of $Al_{14}B_4O_{33}$ were also determined. The amount of Al in the composite powder was determined by ICP AES.[10] The coated samples were then hot pressed under the same conditions as the first set of samples (Table 2).

The third set of samples was produced from the B_6O powder mixed with two different amounts of resin (carbon source). For this, 5 and 10 vol.% phenolic resin were added prior to the hot pressing (Table 3). The weight loss during the pyrolysis of the resin was 2.2 and 4.5%, respectively, so that the carbon content in the sample before hot pressing was 2.8 and 5.5%, respectively. In these samples some Al_2O_3 impurities were found, which were not detected in the pure B_6O materials.

The samples have been named according to their preparation. For example 17-M5.2 is hot pressed B_6O composite with 5.2 wt.% Al powder at 1700 °C; 19-O2.2 is B_6O composite hot pressed at 1900 °C and coated with 2.2 wt.% Al in the form of Al_2O_3; and 19-C5 is hot pressed B_6O composite with 5 wt.% resin at 1900 °C.

The sintered B_6O-based composites were characterised in terms of phase composition using the X-ray diffractometry and scanning electron microscopy. Additionally, the samples were polished and the hardness and fracture toughness were measured. For high magnification images, some of the samples were polished by ion beam.[17]

The fracture toughness (K_{IC}) was measured at indentations with a load of 5 kg. The average of five measured values was used to determine the properties of the B_6O samples. K_{IC} was measured via the DCM method, using Anstis' equation[18] and the determined elastic constants.[9]

The FactSage™ software package was used for the thermodynamic calculations of equilibrium phase compositions. The thermodynamic data were used from the database FACT53 (version 5.3) and the data of B_6O were derived in paragraph 2. The calculations were carried out between 1200 and 2000 °C using the starting composition of the materials assuming 1 wt.% B_2O_3 in the material. In some cases the amount of B_2O_3 was increased

Table 2
Phase composition, density and hardness of hot pressed boron suboxide-based materials from coated powders (crystalline phases in the starting powder B_6O/Al_2O_3) and calculated phases at equilibrium

Material name	Density (g/cm^3)	Vickers hardness, H_{v5} (GPa)	Knoop microhardness (GPa), 500 g	Fracture toughness, K_{IC} ($MPa\,m^{1/2}$)	Crystalline phases formed after sintering	Thermodynamically calculated equilibrium phases at sintering temperature (1900 °C)		Thermodynamically calculated equilibrium phases after cooling
						Solid	Liquid	
19-O2.2	2.52	29.3 ± 0.5	31.1 ± 0.4	3.1 ± 0.1	B_6O, $Al_{18}B_4O_{33}$	B_6O, $Al_{18}B_4O_{33}$	B_2O_3/Al_2O_3	B_6O, $Al_{18}B_4O_{33}$ $Al_4B_2O_9$
19-O3.7	2.45	28.2 ± 1.6	30.2 ± 0.6	3.2 ± 0.2	B_6O, $Al_{18}B_4O_{33}$	B_6O, $Al_{18}B_4O_{33}$	B_2O_3/Al_2O_3	B_6O, $Al_{18}B_4O_{33}$ $Al_4B_2O_9$
19-O5.6	2.51	27.8 ± 1.1	28.6 ± 0.5	3.4 ± 0.1	B_6O, $Al_{18}B_4O_{33}$	B_6O, $Al_{18}B_4O_{33}$	B_2O_3/Al_2O_3	B_6O, $Al_{18}B_4O_{33}$ $Al_4B_2O_9$

Table 3
Properties of the hot pressed B_6O samples made by adding phenolic resin

Material name	Density (g/cm^3)	Vickers hardness, H_{v5} (GPa)	Fracture toughness, K_{IC} ($MPa\,m^{1/2}$)	Crystalline phases formed after sintering	Thermodynamically calculated equilibrium phases after cooling
19-C5	2.46	24.7 ± 0.6	5.25 ± 0.78	B_6O, $Al_{18}B_4O_{33}$	B_6O, B_4C, $Al_{18}B_4O_{33}$
19-C10	2.41	21.5 ± 0.77	5.48 ± 0.58	B_6O, $Al_{18}B_4O_{33}$, B_4C	B_6O, B_4C, $Al_{18}B_4O_{33}$

or decreased to test how stable the solutions are. The calculation was done by minimization of the Gibbs energy of the system using the EQUILIB module of the program FactSage 5.5.

4. Results

In the first set of materials, B_6O powders were admixed with aluminium metal. The aim of this study was to eliminate the existing amorphous B_2O_3 on the surfaces of B_6O powder, which could be a possible reason of the low fracture toughness of B_6O sintered compacts described in the literature. Table 1 shows the Knoop microhardness of the hot pressed samples as well as the calculated equilibrium phases at sintering temperatures. The densities obtained were lower compared to the density obtained for pure B_6O sintered compact. The secondary phase after sintering was $Al_{18}B_4O_{33}$. The two possible phases, $Al_{18}B_4O_{33}$ and $Al_4B_2O_9$ cannot be distinguished by XRD non-ambiguously because the main peaks of both phases are quite similar and the phase content is low. The conclusion of the formation of $Al_{18}B_4O_{33}$ was drawn on the basis of detailed analysis of the microstructure of material 19-O5.6 using TEM[17] which allows the differentiation between the two phases.

When the amount of Al metal was increased to 7.3 wt.%, an additional phase, Al_2O_3, was identified using XRD. In contrast, phases calculated at equilibrium were AlB_{12} and Al_2O_3.

Table 2 shows the properties of the second set of experiments where B_6O powders were coated with Al_2O_3 via CVD. In the coated powders Al_2O_3 was observed besides B_6O. $Al_{18}B_4O_{33}$ phase was identified after sintering. Thus, the Al_2O_3 phase observed on the coated powder disappeared after sintering at 1900 °C. These results agree with the thermodynamically calculated equilibrium phase composition given in Table 2 for the hot pressing temperature 1900 °C and room temperature. The results of the thermodynamic calculations indicate an oxide liquid containing Al_2O_3 and B_2O_3 co-existing at sintering temperatures with B_6O and $Al_{18}B_4O_{33}$. This liquid could recrystallise to form Al_2O_3–B_2O_3 compounds during cooling and the type of aluminium borate formed would depend on the ratio of Al_2O_3 to B_2O_3 in the liquid (Fig. 2). Additionally, the amount of Al_2O_3 and B_2O_3 in the starting composition will strongly change the amount of liquid phase existing during sintering and hence affect densification of sintered materials.

The data in Tables 1 and 2 showed that the addition of Al_2O_3 or Al results in an increase in the fracture toughness in comparison to the pure B_6O materials produced in this work and in comparison to literature data.[1,2] The mechanism of increasing fracture toughness will be discussed elsewhere.[17]

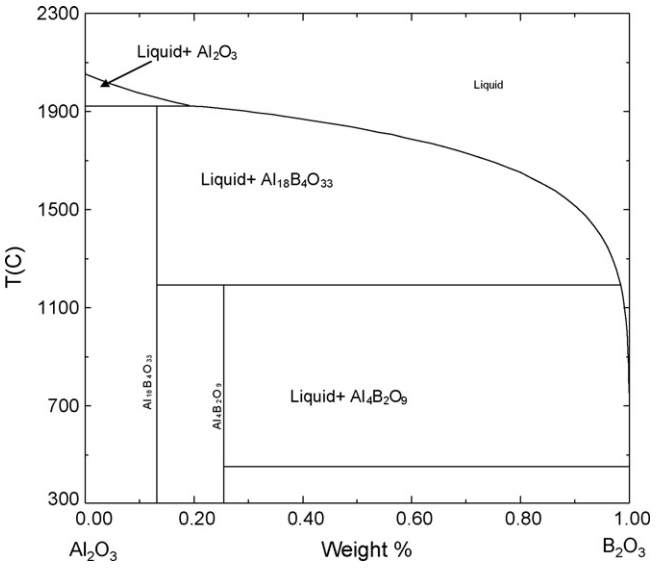

Fig. 2. Calculated phase diagram of Al_2O_3–B_2O_3 system. This diagram completely agree with the diagram given in the ACerS-NIST phase equilibrium diagrams.[20].

Table 4 shows the properties of pure B_6O sample ($19B_6O$) and CVD coated B_6O sample (19-O5.6) which has been annealed after hot pressing at 1900 °C. The analysis of the heat-treated samples showed that the $19B_6O$ sample was stable up to 1900 °C with slight decomposition. 3.5% mass loss was measured for this sample. For the 19O5.6 samples, a mass loss of 11% was observed. Fig. 3 shows the optical images of the cross sections of annealed samples at 1900 °C. When comparing the SEM images of 19-O5.6 before and after annealing, it was observed that the amount of the secondary phase ($Al_{18}B_4O_{33}$) had decreased, especially in the near surface area. Comparing SEM images of 19-O5.6 sample before and after heat treatment at 1900 °C (Fig. 4), the Al containing compound was decomposed extensively.

Table 3 shows the properties of the third set of materials, where B_6O powders were mixed with phenolic resin as a source of carbon. The reason for adding carbon was to cause the carbon to react with B_2O_3 to form B_4C, which could reduce the B_2O_3-

Table 4
Density and weight losses of hot pressed B_6O samples

Sample name	Annealing conditions	Density (g/cm3)	Weight loss (%)
$19B_6O$	As hot pressed	2.51	–
	1900 °C	2.47	3.5
19-O5.6	As hot pressed	2.51	–
	1900 °C	2.30	11

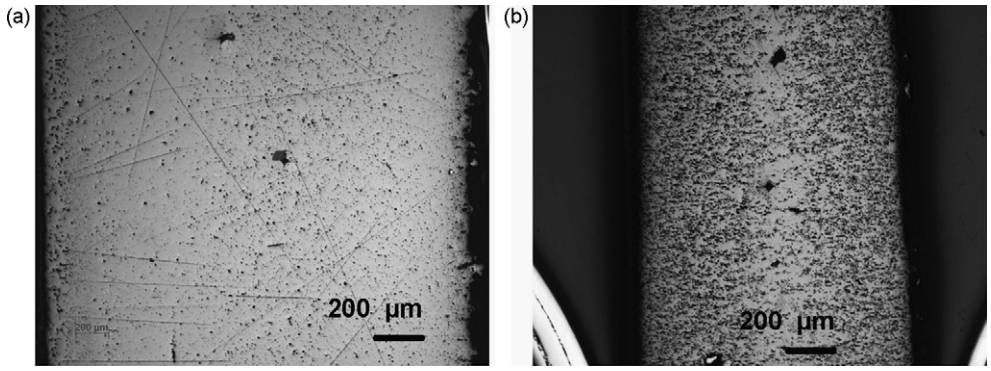

Fig. 3. Optical images of cross-sections of samples annealed at 1900 °C. (a) 19B_6O; (b) 19-O5.6 wt.% Al.

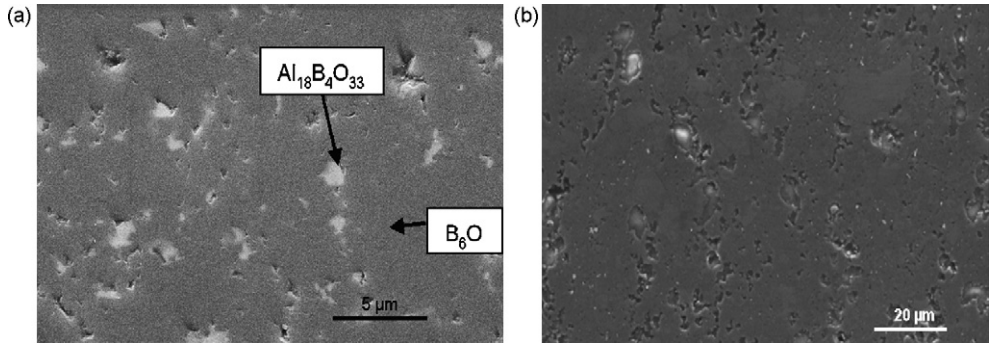

Fig. 4. SEM images of polished cross sections of B_6O composite 19-O5.6 wt.% before heat treatment and (a) edge of the sample after heat treatment at 1900 °C.

content and may prevent grain growth of B_6O during sintering. The B_6O powder used for this set of experiments contain some alumina borate from the alumina boat used during synthesis of the B_6O feedstock. In the sample 19-C5, no B_4C or carbon containing phase was identified using XRD. Nevertheless, B_4C was identified in the 19-C10 sample (Fig. 5). The samples had a slightly lower density than the samples sintered with Al_2O_3. Especially the material with 10% resin shows an incomplete densification. The material has additionally a lower hardness but higher fracture toughness. This could be connected with the residual porosity. More detailed investigations are necessary to understand this behaviour.

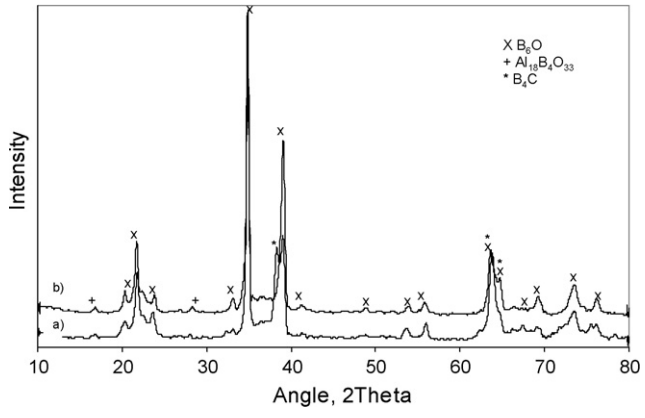

Fig. 5. XRD pattern of the hot pressed 19-C5 (a) and 19-C10 (b).

5. Discussion

5.1. Comparison of experimentally observed and thermodynamically calculated phase compositions

The thermodynamic calculations and the experimental data show that Al_2O_3 or Al-borates are in equilibrium with the B_6O. Aluminium will react with B_2O_3 or B_6O to form Al_2O_3. The existing B_2O_3 on the surface of the powder and the Al_2O_3 added formed aluminium borates, and at high temperature an oxide liquid. This liquid would contain B_2O_3/Al_2O_3 and some B_6O. According to the phase diagram (Fig. 2) a liquid phase is formed at 1200 °C if the Al_2O_3/B_2O_3 mol ratio is between 9:2 and 2:1. All secondary phases are solved in the liquid at the incongruent melting point of $Al_{18}B_4O_{33}$. The detailed analysis of the microstructure using TEM[17] and of ion beam polished samples (Fig. 6) showed that, beside the crystalline phases B_6O and $Al_{18}B_4O_{33}$, a boron rich amorphous phase is formed, indicating, that the B_2O_3/Al_2O_3 ratio is in the indicated area. The existence of the boron rich amorphous phases, which partially decomposes under the preparation conditions, can be shown by comparing the prepared samples with BN samples prepared under similar conditions (Fig. 6). In both cases between the grains of the crystalline phase boron and oxygen rich phases are found.[19]

From these data it could be concluded, that the $Al_4B_2O_9$ phase, which crystallises from the liquid phase during cooling only at low temperatures (below 1200 °C) does not form for kinetic reasons and a boron rich residual amorphous grain boundary is formed beside $Al_{18}B_4O_{33}$.

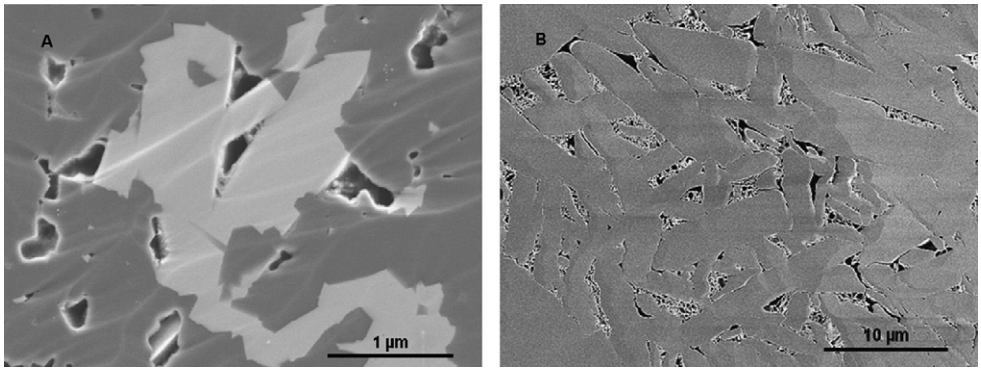

Fig. 6. FESEM micrograph of the ion beam polished sample 19-O5.6 (a) and of hBN material (b) prepared in the same way.

In the case of the materials of the second (Al_2O_3-additive) and third set of experiments (carbon additions), the calculated and observed phases are in good agreement.

For the first set of samples, which were produced by the mixture of Al and B_6O, the same borate phase was observed beside B_6O as in the second set of samples, showing the reaction of Al with B_2O_3 or B_6O. The phases calculated at equilibrium were AlB_{12} and Al_2O_3. The thermodynamic calculations of the phase equilibrium between 1200 and 2000 °C showed the formation 10 wt.% AlB_{12}. Experimentally AlB_{12} was not observed, beside the fact that some of the intensive peaks of the XRD pattern of AlB_{12} do not overlap with B_6O and the determination of AlB_{12} could be possible. The difference between the thermodynamic calculations and the experimental results could be attributed on the one hand to the fact that during processing the aluminium picked up some oxygen. On the other hand, the Al can react with B_6O reducing the oxygen content in the B_6O due to the existence of the non-stoichiometry of B_6O, i.e.

$$3B_6O + 2xAl \Rightarrow xAl_2O_3 + 3B_6O_{(1-x)} \quad (3)$$

An indication for such a reaction was found by analysing the lattice parameter of B_6O powders and sintered samples. Detailed XRD analysis of the samples made with addition of Al_2O_3 had shown that the lattice parameter of B_6O changes from $a = 0.5370 \pm 0.0001$ nm to 0.5390 ± 0.0001 nm in the sintered samples without additives and also with Al_2O_3 additions.[9] This indicates that some additional oxygen was incorporated into the B_6O lattice during densification. In[16] it was shown that the oxygen content can strongly vary with the temperature of synthesis of B_6O. Assuming the reduction of the oxygen content of B_6O, the formation of AlB_{12} would no more be expected. But this would still not explain the formation of aluminium borates, because this would necessitate the stability of B_2O_3 also. As it was mentioned before, the determination of B_2O_3 in the starting powder is complicated, but calculations with B_2O_3 contents of up to 3 wt.% yielded unchanged results. The possible explanation could be: The area of coexistence of Al_2O_3 and $Al_{18}B_4O_{33}$ depends on the non-stoichiometry of B_6O_{1-x}. For low oxygen content (high x values) it could be in equilibrium with Al_2O_3 and for high oxygen content with $Al_{18}B_4O_{33}$. Such behaviour is quite common for phases with a homogeneity region. Additionally, the calculations do not take into account the solubility of B_6O in the liquid phase. If the composition of the liquid in equilibrium with B_6O_{1-x} is more B_2O_3 rich, the composition of B_6O would not change completely to the equilibrium ones during cooling. Further investigations of the phase equilibria are necessary to understand this.

The thermodynamic calculations showed that at low temperatures, carbon is in equilibrium with the B_6O and reacts with B_2O_3 forming B_6O:

$$8C + 3B_2O_3 = B_6O + 8CO \quad (4)$$

This reaction strongly depends on the CO-partial pressure and therefore the stability of the liquid B_2O_3 during sintering strongly depends on transport of CO. At 1544 °C, the CO partial pressure reaches 1 atm resulting in strong reduction of the B_2O_3 in a system with a fixed pressure of 1 atm.

Carbon can react also with B_6O:

$$2B_6O + 5C = 3B_4C + 2CO \quad (5)$$

The formed CO partial pressure is lower than the equilibrium pressure of reaction (4). Therefore the reaction takes place only after decomposition of B_2O_3.

At 1616 °C, the CO partial pressure of reaction (5) reaches 1 atm and carbon strongly reduces B_6O forming B_4C and CO. The added carbon therefore reduces on the one hand B_2O_3 and evaporates as CO and, on the other hand forms B_4C. The fact that for the sample with the low carbon content the formation of B_4C could not be determined is the result of the consumption of carbon by the formation of CO and reduction of B_2O_3. The CO partial pressures of the two reactions as a function of the temperature are shown in Fig. 7. The areas of the stability of the different phases are shown, which are separated by the lines.

Even if the thermodynamic calculations suggest that B_4C would be decomposed at low temperatures, this would be unlikely to happen during cooling or heating due to kinetic reasons. Therefore the use of B_4C in B_6O/B_4C composites will result in more reproducible results of sintering due to reduced interaction. This means that regardless of the starting composition, B_6O and B_4C phases would be present at the sintering temperature (1900 °C) except when the overall pressure in the system is increased, for instance, to 10 atm. In such a condition, C could be stable at sintering temperature and B_4C only forms at about 1925 °C.

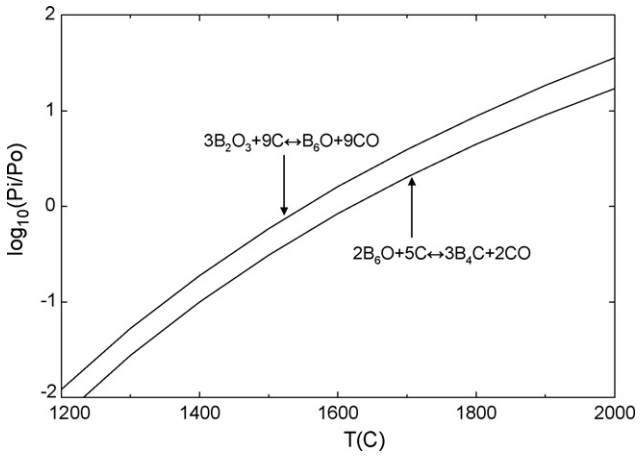

Fig. 7. Partial pressure of CO for the two solid systems, $B_6O/B_2O_3/C$ and $B_6O/B_4C/C$.

5.2. Decomposition at high temperatures and sintering

In Fig. 8 the calculated compositions of the gas phase as a function of temperature are given for B_6O/B_2O_3 and for $B_6O/B_2O_3/Al_2O_3$ compositions. Two things can be derived from these calculations. The addition of Al_2O_3 lowers the partial pressure of the boron-containing compounds by a factor of 2 at sintering temperature (compare Fig. 8a and b). This helps to stabilize the liquid phase during sintering. The role of Al_2O_3-addition is to reduce the activity of B_2O_3 in the oxide melt and therefore the partial pressures.

Independently on the drop of the partial pressures due to the addition of Al_2O_3 the partial pressures of Al and boron containing species are still high ($AlBO_2$ partial pressure is 4.1×10^{-4} atm and $(BO)_2$ are in the range of 10^{-2} atm at 1900 °C). This causes a strong decomposition of the liquid phase by simple evaporation of B_2O_3 and by interaction with B_6O. This reaction can be summarised as:

$$2B_6O + 5(Al_2O_3 + B_2O_3)\,\text{liquid} \Rightarrow 6(BO)_2 + 10BAlO_2 \quad (6)$$

The partial pressure of $(BO)_2$ is higher than that of $AlBO_2$ therefore the liquid/grain boundary phases will be enriched with Al_2O_3 during sintering. Under the heat treatment conditions the evaporation is so intensive that nearly the complete grain boundary phase evaporates, resulting in the low density and high porosity. These high partial pressures make it complicated to densify the material without external pressure.

The $(BO)_2$ and B_2O_3 have the highest partial pressure in the system B_6O/B_2O_3. The first is formed due to the interaction between B_6O and B_2O_3. The second is caused by simple evaporation of B_2O_3. After the decomposition of B_2O_3 existing in the pockets between the B_6O grains, the partial pressure drops and

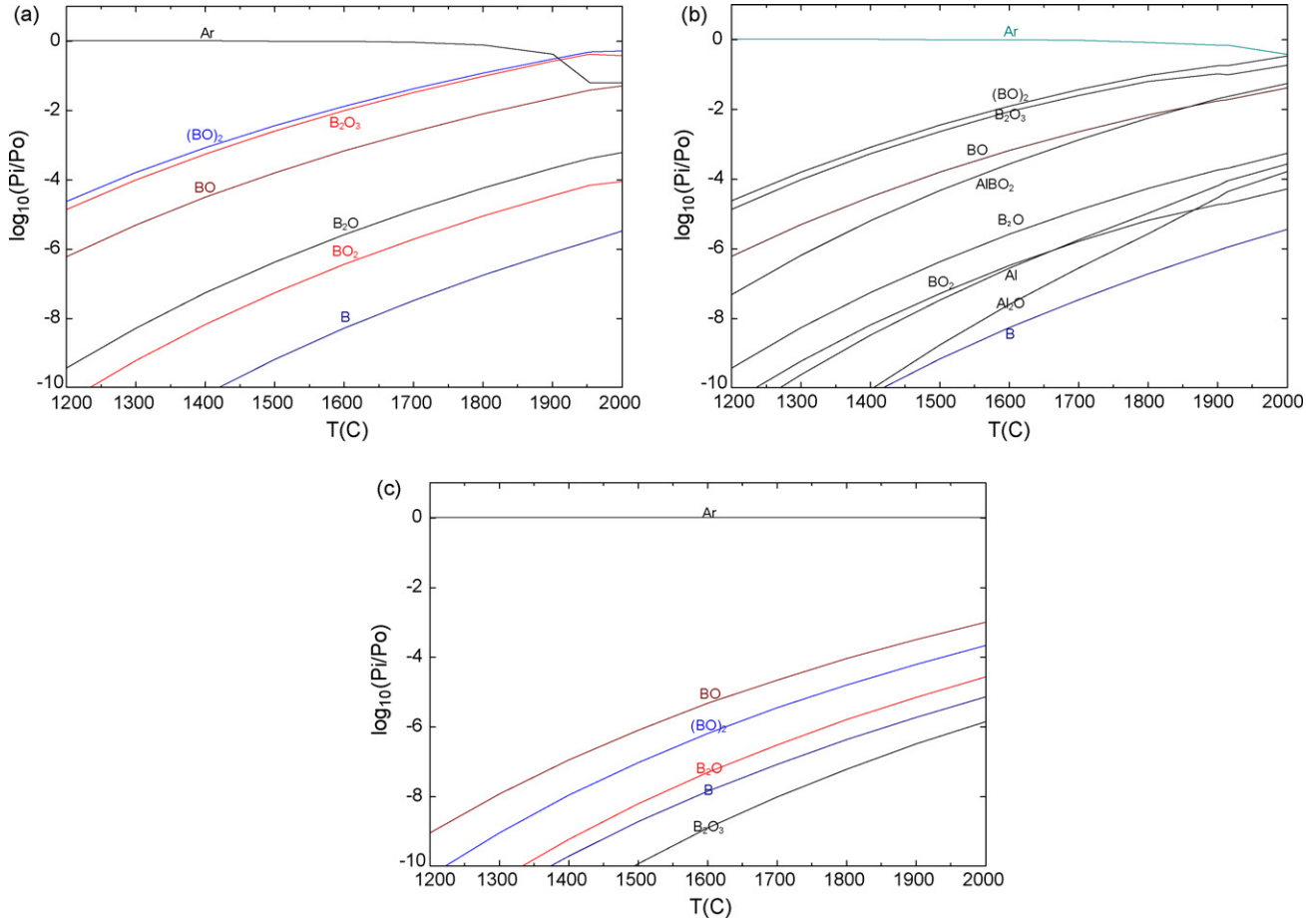

Fig. 8. Composition of the gas phase for materials (a) B_6O–2 wt.% B_2O_3; (b) B_6O–4 wt.% Al_2O_3–2 wt.% B_2O_3 and for (c) pure B_6O.

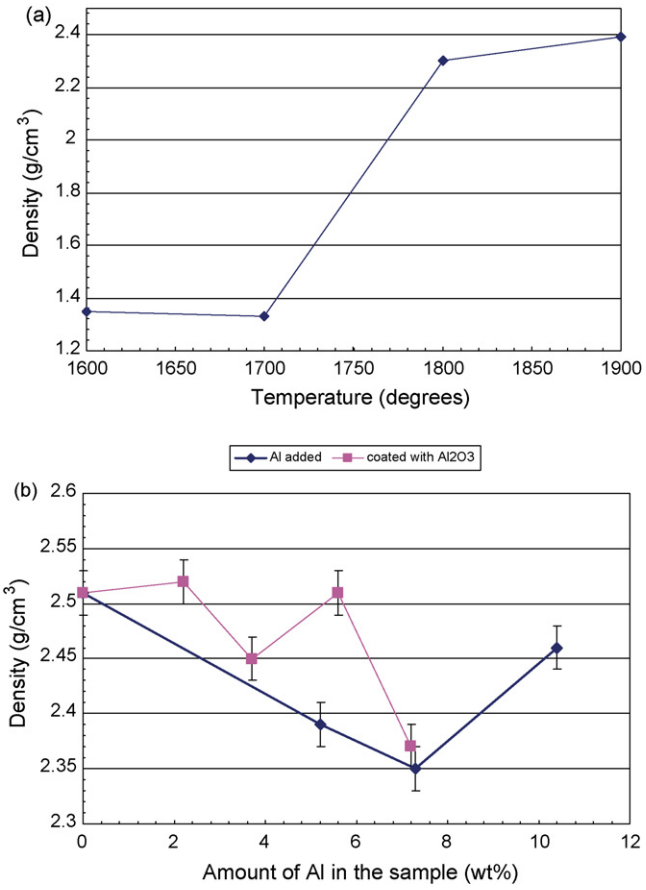

Fig. 9. Densities of hot pressed B_6O samples (with 5.2 wt.% Al) as a function of sintering temperature. (a) Density of B_6O samples hot pressed at 1900 °C as a function of the amount of Al added, and the amount of Al in the coated samples (coating consists of Al_2O_3) (b).

the decomposition will strongly be retarded (see Fig. 8a and c). Therefore the heat treatment of the pure B_6O results in a relative low weight loss and only a small reduction of the density.

Fig. 9a shows the graph of the density as a function of temperature for the coated B_6O with 5.2 wt.% Al additive and Fig. 9b shows the graph of density as a function of the amount of Al added for B_6O composites (first and second set of materials (Tables 1 and 2). The hot pressed B_6O materials with Al_2O_3 coating up to 5.6 wt.% Al showed some scattering of the reached densities. The densities of the samples with the lowest amount of Al (19-O2.2) had a highest density, 2.52 g/cm^3. The sample with highest amount of Al (19-O7.2) had the lowest density, 2.37 g/cm^3.

Thermodynamic calculations of the amount of liquid in the material as a function of the Al_2O_3 content in the material (Fig. 10) showed that changes in the B_2O_3 and Al_2O_3 content strongly affect the amount of liquid phase formed at different temperatures and hence strongly influence the densification. It has to be mentioned that the calculation of the amount of liquid phases do not take into account the solubility of B_6O in the liquid. Therefore this information can only be used for the qualitative explanation of the sintering behaviour. Decreasing amount of B_2O_3 at constant Al_2O_3 content reduces the amount of liquid existing during sintering at lower temperatures. The amount of

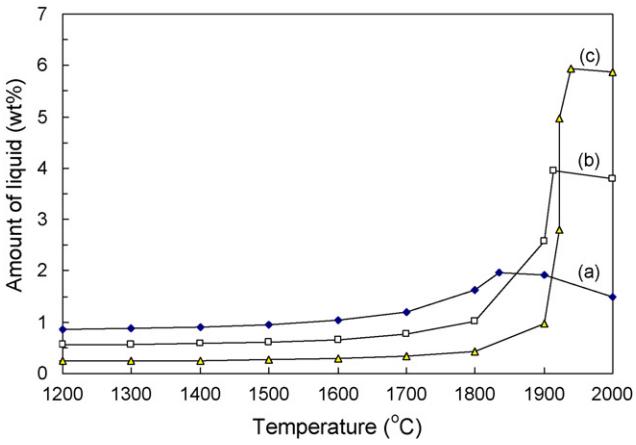

Fig. 10. Amount of liquid phase as function of temperature and ratio of B_2O_3/Al_2O_3. (a) 1:1; (b) 1:3; (c) 1:5. Concentration of B_2O_3 is 1 wt.%.

liquid phase strongly increases with increasing temperature due to the increased solubility of $Al_{18}B_4O_{33}$ in the liquid, which melts at 1950 °C. This is consistent with the calculated phase diagram (Fig. 2) and the experimental phase diagrams.[20] At temperatures above the melting point of $Al_{18}B_4O_{33}$ the amount of liquid decreases due to the enhanced evaporation of the liquid phase. Therefore only a small temperature interval exists for densification. With increasing Al_2O_3 content at constant B_2O_3 content, the amount of liquid phase reduces due to the formation of higher amount of $Al_{18}B_4O_{33}$. At constant Al_2O_3 the increase of the amount of B_2O_3 will increase the amount of liquid phase, but also the partial pressures of B_2O_3 and $(BO)_2$ increases resulting in higher decomposition. Additional it will result in an unstable, very soft boron oxide rich amorphous grain boundary phase. Therefore this would not be an option for improving the sintering behaviour.

The addition of Al reduces, at least partially, the amount of B_2O_3 in the material. Therefore the density of materials with added metallic Al strongly reduces with increasing Al content. For the sample with very high amounts of Al_2O_3 (10.4 wt.% Al, i.e. with nearly 20 wt.% Al_2O_3) the density increases slightly. This could be caused by the higher density of Al_2O_3 and the high amount of Al_2O_3 which sinters normally at much lower temperatures. Nevertheless this material is still porous.

These results suggest that the mechanism of densification of the materials is that of liquid phase sintering. Also the microstructural figures support this finding (Figs. 4 and 6) as well as TEM investigations carried out and published elsewhere.[17]

Further improvement of the material is possible by reducing the grain size and optimizing the hot pressing parameter especially the pressure and the isothermal holding time.

6. Conclusion

B_6O composites were prepared by hot pressing of B_6O powder with alumina, aluminium and carbon additions. Dense materials were achieved at 1900 °C. The resulting materials have increased fracture toughness in comparison to the pure B_6O samples and nearly the same hardness as pure B_6O composites.

Thermodynamic properties of B_6O have been estimated up to 2300 K and validated using the secondary phases formed in the investigated materials. The data allow the prediction of the stability of the liquid and crystalline phases. Therefore they can form the basis for the search of new sintering additives that would allow the sintering of the composites at lower temperatures. Thermodynamic calculations of B_6O composites and the observed microstructure support the conclusion that the mechanism of densification of the B_6O/Al_2O_3 composites is, at least predominantly, liquid phase sintering. The experimental, as well as the calculated results, reveal that the densification depends strongly on the composition of the starting materials, with B_2O_3 normally present on the surfaces of starting B_6O particles playing a major role in the densification and hence the hardness and fracture toughness of the sintered composites.

References

1. Hubert, H., Garvie, L., Devouard, B., Buseck, P., Petuskey, W. and McMillan, P., *Chem. Mater.*, 1998, **10**, 1530–1537.
2. Itoh, H., Maekawa, I. and Iwahara, H., High pressure sintering of B_6O powder and properties of the sintered compact. *J. Soc. Mater. Sci. Jpn.*, 1998, **47**(10), 1000–1005.
3. He, D., Akaishi, M., Scott, B. L. and Zhao, Y., Growth of boron suboxide crystals in the B–B_2O_3 system at high pressure and high temperature. *J. Mater. Res.*, 2002, **17**(2), 284–290.
4. Garvie, L. A. J., Hubert, H., Petuskey, W. T., McMillan, F. P. and Buseck, P. R., High-pressure, high-temperature syntheses in the B–C–N–O system. II. Electron energy-loss spectroscopy. *J. Solid Sate Chem.*, 1997, **133**, 365–371.
5. Yu, S., Wang, G., Yin, S., Zhang, Y. and Liu, Z., Nanostructured films of boron suboxide by pulse laser deposition. *Phys. Lett. A*, 2000, **268**, 442–447.
6. Hubert, H., Devouard, B., Garvie, L. A. J., O'Keeffe, M., Buseck, P. R., Petuskey, W. T. *et al.*, Icosahedral packing of B12 icosahedra in boron suboxide (B_6O). *Nature*, 1998, **39**, 376–378.
7. Davis G. J., Sigalas, I., Herrmann, M. and Shabalala, T., PCT/IB2006/002456, 2006.
8. Ellison-Hayashi, C., Zandi, M., Murray, Csillag, F. J. and Kuo, S.-Y., US Patent 5, 135, 892, 1992.
9. Shabalala, T. C., The preparation and characterisation of boron suboxide (B_6O) based composites. PhD thesis, University of the Witwaterstand, 2007.
10. Shabalala, T. C., Mclachlan, D. S., Sigalas, I. J. and Herrmann, M., Hard and tough boron suboxide based composites. *Ceram. Int.*, in press, available online at www.sciencedirect.com.
11. Makarov, V. S. and Ugai, Y. A., Thermochemical study of boron suboxide B_6O. *J. Less-Comm. Met.*, 1986, **117**, 277–281.
12. Tsagareishvili, G. V., Tsagareishvili, D. Sh., Tushishvili, M. Ch., Omiadze, I. S., Naumov, V. N. and Tagaev, A. B., Enthalpy and heat capacity of boron suboxide in the temperature range of 298.15–781.8 K. In *USSR, AIP Conference Proceedings, Vol. 231 (Boron-Rich Solids)*, 1991, pp. 384–391 (in Russian).
13. Naumov, V. N., Tagaev, A. B., Tsagareishvili, D. Sh., Tsagareishvili, G. V. and Tushishvili, M. Ch., Thermodynamic properties of boron suboxide in the temperature range 11.44–311.84 K. In *USSR, Soobshcheniya Akademii Nauk Gruzinskoi SSR, Vol. 138, No. 2*, 1990, pp. 321–324 (CODEN: SAKNAH; ISSN: 0002-3167).
14. *SGPS-SGTE Pure Substances Database*. Scientific Group Thermodata Europe, 2000.
15. Gaskell, D. R., *Introduction to the Thermodynamics of Materials* (*4th edition*). McGraw-Hill Book Company, New York, NY, London, 1981, p. 110.
16. Olofsson, M. and Lundström, T., Synthesis and structure of non-stoichiometric B_6O. *J. Alloys Compd.*, 1997, **257**, 91–95.
17. Kleebe, H.-J., Lauterbach, S., Shabalala, T. C., Herrmann, M. and Sigalas, I., B6O: a correlation between mechanical properties and microstructure evolution upon Al2O3 addition during hot-pressing, *J. Am. Ceram. Soc.*, in press.
18. Anstis, G., Chantikul, P., Lawn, B. and Marshall, D., A critical evaluation indentation techniques for measuring fracture toughness. I. Direct crack measurements. *J. Am. Ceram. Soc.*, 1981, **64**, 533–538.
19. S. Hoehn, Private Communication, IKTS, Dresden.
20. *ACerS-NIST Phase Equilibrium Diagrams, CD-ROM Database Version 3.1*, 2005.